

Functional Characterization of *Burkholderia pseudomallei* Trimeric Autotransporters

Cristine G. Campos, Matthew S. Byrd, Peggy A. Cotter

Department of Microbiology and Immunology, University of North Carolina School of Medicine, Chapel Hill, North Carolina, USA

Burkholderia pseudomallei is a tier 1 select agent and the causative agent of melioidosis, a severe and often fatal disease with symptoms ranging from acute pneumonia and septic shock to a chronic infection characterized by abscess formation in the lungs, liver, and spleen. Autotransporters (ATs) are exoproteins belonging to the type V secretion system family, with many playing roles in pathogenesis. The genome of *B. pseudomallei* strain 1026b encodes nine putative trimeric AT proteins, of which only four have been described. Using a bioinformatic approach, we annotated putative domains within each trimeric AT protein, excluding the well-studied BimA protein, and found short repeated sequences unique to *Burkholderia* species, as well as an unexpectedly large proportion of ATs with extended signal peptide regions (ESPRs). To characterize the role of trimeric ATs in pathogenesis, we constructed disruption or deletion mutations in each of eight AT-encoding genes and evaluated the resulting strains for adherence to, invasion of, and plaque formation in A549 cells. The majority of the ATs (and/or the proteins encoded downstream) contributed to adherence to and efficient invasion of A549 cells. Using a BALB/c mouse model of infection, we determined the contributions of each AT to bacterial burdens in the lungs, liver, and spleen. At 48 h postinoculation, only one strain, Bp340::pDbpaC, demonstrated a defect in dissemination and/or survival in the liver, indicating that BpaC is required for wild-type virulence in this model.

Burkholderia pseudomallei is a Gram-negative soil saprotroph and the causative agent of melioidosis, a severe and often systemic infection that can occur in both chronic and acute forms (1, 2). Acute pulmonary melioidosis is characterized by high fever, respiratory distress, and the formation of visceral abscesses, while chronic pulmonary melioidosis is characterized by prolonged pneumonia and abscess formation in the lungs, liver, and spleen (2). Overall mortality due to melioidosis is high, approaching 50% in Thailand and 20% in Australia (2, 3). *B. pseudomallei* is endemic to Southeast Asia and northern Australia but has also been identified in Africa, South and Central America, India, and the Middle East (4, 5). Intrinsic resistance to clinically important antibiotics, including beta-lactams and many macrolides and aminoglycosides (6, 7), as well as the ability to invade and persist in phagocytic cells (8, 9), contributes to the difficulty in successfully treating *B. pseudomallei* infections. Intense antibiotic therapy over several months is often required to eliminate this bacterium, but despite a robust treatment regimen, relapse occurs at a high frequency (10).

B. pseudomallei is able to adhere to and invade a variety of epithelial cell lines and has also been shown to invade and survive within macrophage-like cells (8, 11–14). Following uptake by a eukaryotic cell, *B. pseudomallei* is able to escape the endocytic compartment and enter the cytoplasm by using one of its type III secretion systems (T3SS). Once in the cytoplasm, the bacterium polymerizes host actin using the surface protein BimA to move within host cells, avoiding exposure to the extracellular space (9, 15). *B. pseudomallei* can induce fusion of neighboring host cell membranes, leading to the formation of multinucleated giant cells (MNGC), in a process that depends on one of its type VI secretion systems (T6SS) (9, 16–18). Although several putative *B. pseudomallei* adhesins have been identified by genomic screens and protein microarrays (19, 20), only a few have been characterized, including type IV pili and two putative autotransporter (AT) proteins, BoaA and BoaB (21, 22).

AT proteins, the largest family of secreted proteins among Gram-negative bacteria, are secreted via the type V secretion system pathway. AT proteins share three common features: an N-terminal signal sequence for Sec-dependent translocation into the periplasm, a central passenger region containing the functional domain(s), and a highly conserved, outer membrane channel-forming β -barrel at the C terminus that is required for export of the passenger domain to the surface (23). The two subfamilies of AT proteins, classical and trimeric, are distinguished by the mechanism of β -barrel assembly and by the processing and localization of the passenger domain (24). The C-terminal β -domains of classical ATs are sufficient to form a channel, while trimeric ATs require three polypeptides to form the outer membrane channel, with each β -domain contributing one-third of the channel (23, 25, 26). In addition, classical AT proteins function as monomers, and cleavage of the passenger domain usually occurs at or near the junction of the β -barrel and passenger domains. Once cleaved, classical ATs remain noncovalently associated with the cell surface or are released into the extracellular environment (23, 24). In contrast, trimeric AT passenger domains remain covalently linked to the β -domain, with the N terminus located distal to the cell surface (23, 25).

AT proteins have been implicated in virulence in numerous

Received 29 April 2013 Accepted 11 May 2013

Published ahead of print 28 May 2013

Editor: S. R. Blanke

Address correspondence to Peggy A. Cotter, pcotter@med.unc.edu.

C.G.C. and M.S.B. contributed equally to this article.

Supplemental material for this article may be found at <http://dx.doi.org/10.1128/IAI.00526-13>.

Copyright © 2013, American Society for Microbiology. All Rights Reserved.

doi:10.1128/IAI.00526-13

TABLE 1 Strains and plasmids used in this study

Strain or plasmid	Description	Source or reference
Strains		
<i>E. coli</i> strains		
DH5 α	Molecular cloning strain	67
RHO3	Conjugation strain; Km ^r Δ asd Δ aphA	32
<i>B. pseudomallei</i> strains		
Bp340	Δ amrRAB- <i>oprA</i> derivative of <i>B. pseudomallei</i> 1026b	33
Bp340::pD <i>boaA</i>	Bp340 with <i>boaA</i> disrupted by pCC1; Km ^r	This study
Bp340::pD <i>boaB</i>	Bp340 with <i>boaB</i> disrupted by pCC2; Km ^r	This study
Bp340::pD <i>bpaA</i>	Bp340 with <i>bpaA</i> disrupted by pCC3; Km ^r	This study
Bp340::pD <i>bpaB</i>	Bp340 with <i>bpaB</i> disrupted by pCC4; Km ^r	This study
Bp340::pD <i>bpaC</i>	Bp340 with <i>bpaC</i> disrupted by pCC5; Km ^r	This study
Bp340::pD <i>bpaD</i>	Bp340 with <i>bpaD</i> disrupted by pCC6; Km ^r	This study
Bp340::pD <i>bpaE</i>	Bp340 with <i>bpaE</i> disrupted by pCC7; Km ^r	This study
Bp340::pD <i>baaE</i>	Bp340 with <i>baaE</i> disrupted by pCC7; Km ^r	This study
Bp340::pD <i>bpaF</i>	Bp340 with <i>bpaE</i> disrupted by pCC8; Km ^r	This study
Bp340 Δ <i>boaB</i>	Bp340 with an in-frame, nonpolar <i>boaB</i> deletion	This study
Bp340 Δ <i>bpaE</i>	Bp340 with an in-frame, nonpolar <i>bpaE</i> deletion	This study
Bp340 Δ <i>bpaF</i>	Bp340 with an in-frame, nonpolar <i>bpaF</i> deletion	This study
Bp340 Δ <i>baaFG</i>	Bp340 with an in-frame, nonpolar <i>baaFG</i> deletion	This study
Plasmids		
pEXKm5	Allelic exchange vector; Ap ^r Km ^r <i>sacB</i> ⁺ <i>gusA</i> ⁺	32
pCC1	pCC with a 420-bp internal fragment of <i>boaA</i> ; Km ^r	This study
pCC2	pCC with a 409-bp internal fragment of <i>boaB</i> ; Km ^r	This study
pCC3	pCC with a 411-bp internal fragment of <i>bpaA</i> ; Km ^r	This study
pCC4	pCC with a 419-bp internal fragment of <i>bpaB</i> ; Km ^r	This study
pCC5	pCC with a 396-bp internal fragment of <i>bpaC</i> ; Km ^r	This study
pCC6	pCC with a 1,716-bp internal fragment of <i>bpaD</i> ; Km ^r	This study
pCC7	pCC with a 434-bp internal fragment of <i>bpaE</i> ; Km ^r	This study
pCC <i>baaE</i>	pCC with a 370-bp internal fragment of <i>baaE</i> ; Km ^r	This study
pCC8	pCC with a 684-bp internal fragment of <i>bpaF</i> ; Km ^r	This study
pCCX3	pEXKm5 with <i>bpaE</i> flanking sequences; Ap ^r Km ^r	This study
pMBX1	pEXKm5 with <i>bpaF</i> flanking sequences; Ap ^r Km ^r	This study
pMBX2	pEXKm5 with <i>baaFG</i> flanking sequences; Ap ^r Km ^r	This study
pMBX3	pEXKm5 with <i>boaB</i> flanking sequences; Ap ^r Km ^r	This study

Gram-negative bacterial pathogens. Two prototypical trimeric ATs, YadA (from *Yersinia enterocolitica*) and Hia (from *Haemophilus influenzae*), function as adhesins, and YadA also confers serum resistance by interfering with complement activation (27, 28). *B. pseudomallei* strain 1026b, isolated from a melioidosis patient in Thailand (29), carries 11 putative AT proteins (2 classical and 9 trimeric proteins). Homologs of the AT-encoding genes have been identified in strain K92643 and are generally well conserved among other *B. pseudomallei* isolates (30). Apart from the host-actin-polymerizing BimA protein, only three *B. pseudomallei* trimeric AT proteins have been described. BoaA and BoaB have been reported to function as adhesins *in vitro* and to contribute to *B. pseudomallei* replication inside macrophage-like cells (21). A portion of the passenger domain of a third AT protein, encoded by *bpaA*, has been crystallized, and the structure of its tightly woven trimeric head region resembles that of other trimeric ATs, including YadA, Hia, and BadA from *Bartonella henselae* (31).

In this study, we investigated eight *B. pseudomallei* trimeric ATs and evaluated their roles in adherence, invasion, and plaque formation *in vitro*. We also performed the first animal experiments using any *B. pseudomallei* strains defective for production of trimeric ATs and found that one trimeric AT, BpaC, is required for efficient dissemination of bacteria to or survival within the liver in a BALB/c mouse respiratory infection model.

MATERIALS AND METHODS

Bacterial strains. All manipulations of *B. pseudomallei* were conducted in a CDC/USDA-approved animal biosafety level 3 (ABSL3) facility at the University of North Carolina at Chapel Hill. The bacterial strains used in this study are listed in Table 1. *B. pseudomallei* strains were cultured in low-salt lysogeny broth (LSLB; 10 g/liter tryptone, 5 g/liter yeast extract, 2.5 g/liter NaCl) or on LSLB agar (Sigma-Aldrich, St. Louis, MO) for 24 h at 37°C. *Escherichia coli* strains were grown in LB (10 g/liter tryptone, 5 g/liter yeast extract, 10 g/liter NaCl) or on LB agar. Where appropriate, culture media were supplemented with kanamycin (Km; 125 μ g/ml for *B. pseudomallei* and 50 μ g/ml for *E. coli*). LB agar was supplemented with 400 μ g/ml of diaminopimelic acid (DAP; LL-, DD-, and *meso*-isomers; Sigma-Aldrich, St. Louis, MO) to support growth of RHO3 cells (32). Yeast extract-tryptone (YT; 10 g/liter of yeast extract and 10 g/liter of tryptone) medium supplemented with 15% sucrose and X-Gluc (5-bromo-4-chloro-3-indolyl- β -D-glucuronic acid; GoldBio, St. Louis, MO) was used for counterselection during the construction of *B. pseudomallei* deletion mutant strains (32).

Construction of *B. pseudomallei* mutant strains and plasmids. Deletion of the *boaB*, *bpaE*, *bpaF*, and *baaFG* genes from *B. pseudomallei* strain Bp340 (a derivative of strain 1026b containing a Δ amrRAB-*oprA* mutation [33]) was carried out by allelic exchange using pEXKm5 derivatives (32). DNA fragments containing approximately 500 bp 5' of the gene(s) (including the first three codons) and 500 bp 3' of the gene(s) (including the last three codons) were generated using a two-step, overlap PCR approach or were cloned directly into pEXKm5, resulting in plas-

mids pMBX3, pCCX3, pMBX1, and pMBX2. Plasmids were transformed into *E. coli* RHO3 cells and delivered to Bp340 by conjugation (32). Disruption strains were constructed by amplifying an internal fragment within each gene and ligating this fragment into the suicide vector pCC (a derivative of pRE118 [34] created by digesting the plasmid with EcoRI and religating the backbone without the *sacB1* gene). Plasmids were transformed into *E. coli* RHO3 cells and were delivered to Bp340 by conjugation. Primer sequences are provided in Table S1 in the supplemental material, and plasmid construction is also described in detail in the supplemental material.

Bacterial conjugations. Matings between *B. pseudomallei* and *E. coli* strain RHO3 were performed by incubating Bp340 with RHO3 cells carrying the appropriate allelic exchange plasmid or disruption plasmid (Table 1) on LSLB-DAP agar plates overnight. Cointegrants were selected on LSLB containing Km (LSLB/Km). For deletion strains, cointegrants confirmed for plasmid insertion by PCR were grown overnight in LSLB without selection, allowing for a second recombination event to occur and for the plasmid to be lost. An aliquot of cells was plated on YT agar supplemented with 15% sucrose and X-Gluc, as previously described (32). Colonies arising from the counterselection were screened by PCR for the deletion mutation and/or disruption mutation, and all strains were confirmed by DNA sequencing.

Plasmid stability *in vitro*. Strains containing plasmid disruption mutations were grown overnight on LSLB plates containing Km, and single colonies were picked and grown in 10 ml LSLB without Km for 48 h at 37°C. At 24 h and 48 h, an aliquot from each culture was diluted to an optical density at 600 nm (OD₆₀₀) of 0.1, and serial dilutions were plated on LSLB plates with and without Km. Plasmid loss was calculated from the difference in the numbers of colonies on LSLB compared to LSLB/Km. Experiments were performed in triplicate.

Plaque assay. *B. pseudomallei* strains were grown overnight in LSLB at 37°C. Each well of a 6-well plate was seeded with A549 human lung epithelial cells such that confluent monolayers contained approximately 1×10^6 cells per well. Cells were incubated in F12K medium (Cellgro, Circle Westwood, MA) supplemented with 10% fetal bovine serum (FBS; Gibco, Grand Island, NY) at 37°C with 5% CO₂. Bacterial suspensions were diluted to an OD₆₀₀ of 0.1 in fresh tissue culture medium and then further diluted 1:10, and 25 µl of the diluted culture was added to each well (multiplicity of infection [MOI] of 0.1) (35). Plates were incubated for 2 h, and each well was washed thoroughly with fresh culture medium and overlaid with a mixture containing 1.2% low-melting-point agarose (Fisher Scientific, Fairlawn, NJ), F12K with 10% FBS, gentamicin (Gm; 90 µg/ml), and 0.01% neutral red (Fisher Scientific, Waltham, MA). Plates were incubated for 24 h at 37°C with 5% CO₂, and the plaques in each well were enumerated.

Adherence and invasion assays. Bacterial strains and A549 cells were grown as described above. Bacteria were diluted to an OD₆₀₀ of 0.1 in fresh tissue culture medium, and 250 µl of the diluted culture was added to each well of a 6-well plate (MOI of 100) (36). Plates were incubated for 2 h, and each well was washed thoroughly with fresh culture medium. For the adherence assay, cells were immediately lysed using 1% Triton X-100 (Sigma-Aldrich, St. Louis, MO), and lysates were diluted and plated to determine the total number of CFU in each well. For the invasion assay, cells were incubated for an additional 90 min in the presence of Gm (90 µg/ml), washed with fresh culture medium, and lysed using 1% Triton X-100. Lysates were diluted and plated to determine the total number of CFU in each well. To calculate the percentage of adherent or internalized bacteria, the number of adherent or internalized bacteria was divided by the total number of bacteria in the inoculum and multiplied by 100.

Animal experiments. All animal experiments were approved by the Animal Studies Committee of the University of North Carolina at Chapel Hill (protocol 10-165). Six- to 8-week-old female BALB/c mice (The Jackson Laboratory, Bar Harbor, ME) were allowed free access to sterilized food and water. Animals were anesthetized with Avertin (140 mg/kg of body weight; Sigma-Aldrich, St. Louis, MO) by intraperitoneal injection

prior to infection. For all infections, the desired inoculum of *B. pseudomallei* was suspended in phosphate-buffered saline (PBS). Mice were inoculated intranasally with 500 CFU of *B. pseudomallei* and were euthanized by CO₂ overdose at the indicated time points. At least three animals per strain were infected, and some experiments were performed twice and the results combined. Animal experiments were terminated at 48 h, at which time all animals had become moribund. Organs were aseptically harvested and homogenized, and the bacterial burden in each organ was determined by plating serial dilutions of the homogenates.

RESULTS

Bioinformatic characterization of putative trimeric AT-encoding gene loci. Nine putative trimeric AT-encoding genes were identified in the genome of the *B. pseudomallei* clinical isolate 1026b, based on sequences at the 3' ends of the open reading frames (ORFs) that are predicted to encode the characteristic β-domain. The trimeric AT-encoding gene *bimA*, which has been characterized extensively (15, 35), was not included in our analysis. Three of the remaining eight genes were annotated previously, as follows: *boaA* (for *Burkholderia* oligomeric coiled-coil adhesin A), *boaB* (21), and *bpaA* (for *Burkholderia pseudomallei* auto-transporter A) (31). For simplicity, we named the remaining five uncharacterized genes *bpaB* to *-F*. The trimeric AT-encoding genes are distributed between the two *B. pseudomallei* chromosomes: *boaB*, *bpaB*, and *bpaC* are on chromosome I, while *boaA*, *bpaA*, and *bpaD* to *-F* are on chromosome II (Fig. 1).

One or more additional ORFs with unknown functions are present 3' of and in the same orientation as four of the predicted AT genes (*bpaA*, *bpaB*, *bpaE*, and *bpaF*) (Fig. 1). The BP1026B_II1528 ORF, located 3' of *bpaA*, is predicted to encode a protein containing the consensus N-terminal lipobox sequence LGAC but lacking a Lol avoidance signal necessary for retention at the inner membrane, suggesting that this protein is a lipoprotein that is localized to the inner leaflet of the outer membrane (37, 38). The ORFs 3' of *bpaB* and *bpaE* (BP1026B_I2045 or *baaB* [for *Burkholderia* autotransporter-associated protein B] and BP1026B_II0997 or *baaE*, respectively) are predicted to encode OmpA family proteins that share 29% amino acid sequence identity. Like the BP1026B_II1528 gene product, the proteins encoded by *baaB* and *baaE* possess lipobox sequences (LGAC and LTGC, respectively) and are likely localized to the inner leaflet of the outer membrane, given the lack of a Lol avoidance signal. Immediately 3' of *bpaF* is an ORF (BP1026B_II1531) that encodes a hypothetical protein containing domain of unknown function 2827 (DUF2827). DUF2827 proteins are well conserved among *Burkholderia* species, and though a second DUF2827 protein-encoding ORF (BP1026B_II1532) immediately follows the first, the two proteins share only 48% amino acid sequence identity. To distinguish these DUF2827 protein-encoding genes in later analyses, we refer to them as *baaF* and *baaG*.

The first fully sequenced *B. pseudomallei* strain, K92643, was isolated from a patient in Thailand and is the strain in which the 11 autotransporter-encoding genes were first identified (21, 30, 39, 40). Although genes predicted to encode trimeric ATs are conserved among *B. pseudomallei* strains, two of the eight putative AT-encoding genes in our study are annotated differently in strain 1026b compared to K92643. *boaA* (BPSS0796 in K92643) is unannotated in the 1026b genome, but an alignment of the region expected to contain *boaA* with the corresponding region of the K92643 genome shows that *boaA* is indeed present in 1026b and is 91.5% identical to BPSS0796 at the nucleotide level. Similarly,

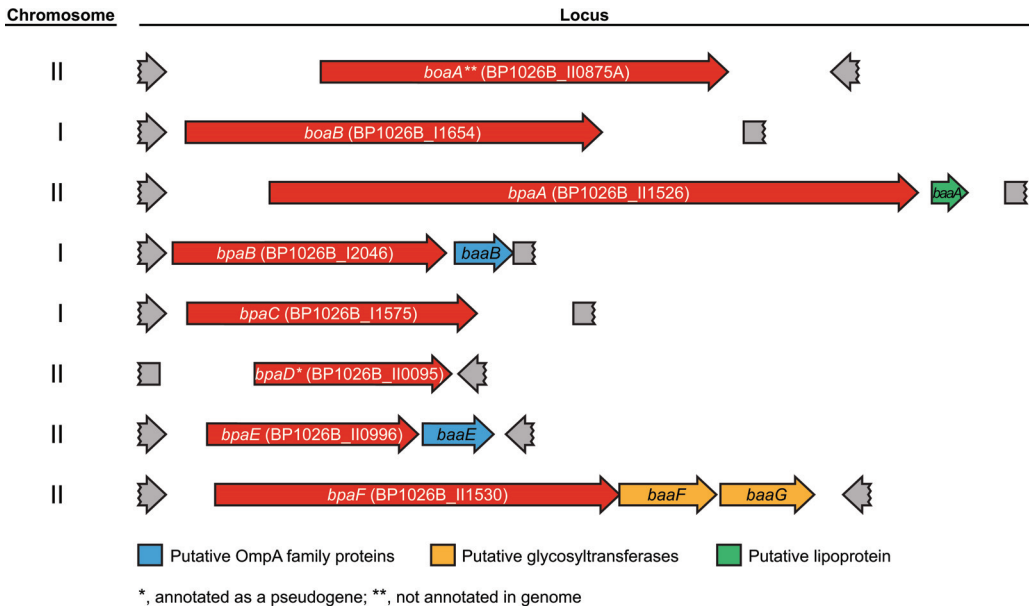


FIG 1 *B. pseudomallei* 1026b putative trimeric AT gene loci. The genomic context of each putative trimeric AT gene is drawn to scale, with the predicted function of immediate 3' genes indicated, if present. The chromosome on which each trimeric AT gene is present is indicated (I or II).

bpaD (BPSS0088 in K92643) is annotated as a pseudogene of 1,833 bp in 1026b; however, aligning the nucleotide sequence 5' of *bpaD* with that of BPSS0088 reveals a full-length *bpaD* gene that is 84.6% identical to BPSS0088 at the nucleotide level.

Bioinformatic characterization of putative trimeric AT proteins. The predicted proteins encoded by *boaA*, *boaB*, and *bpaA* to *-F* range in size from 72.3 kDa (BpaD; 782 amino acids [aa]) to

241.5 kDa (BpaA; 2,575 aa) and share features common to all trimeric ATs, including a 70- to 80-aa C-terminal β -barrel domain and a passenger domain containing numerous short repeated sequences (Fig. 2). Interestingly, seven of the eight trimeric AT proteins (all but BpaD) have a well-conserved 23-aa extended signal peptide region (ESPR) (black regions in Fig. 2) preceding a typical N-terminal signal sequence (dark blue regions in Fig. 2);

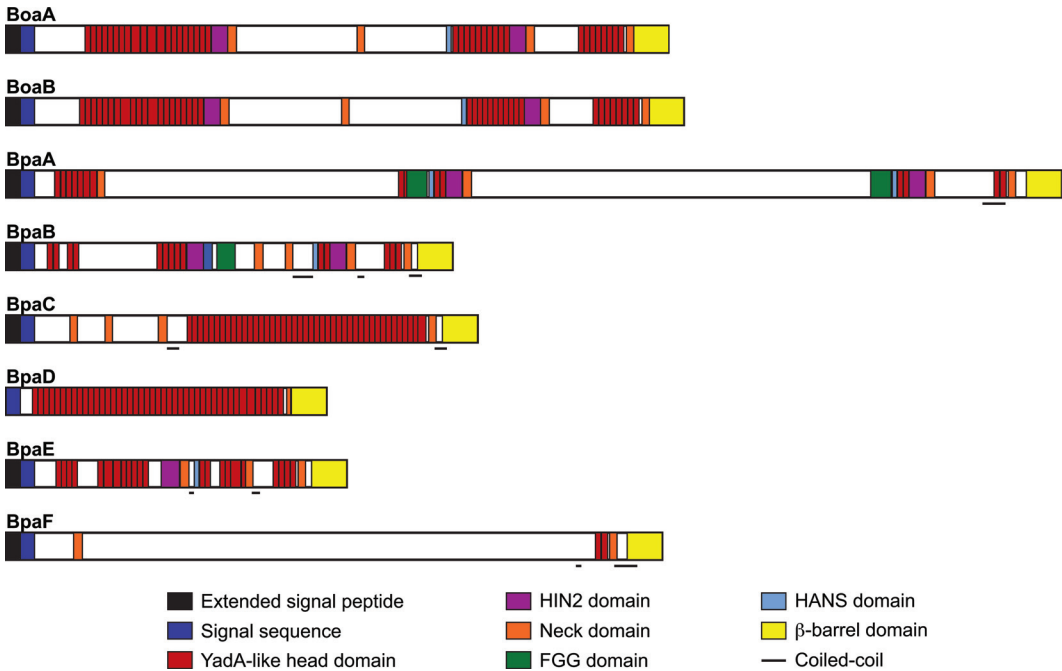


FIG 2 *B. pseudomallei* 1026b putative trimeric AT protein domains. Domains predicted by daTAA (domain annotation of trimeric autotransporter adhesins) are indicated in the legend. The characteristic C-terminal β -barrel domain is shown in yellow, and predicted coiled-coil regions are underlined. White regions are sequences with limited homology to known AT proteins, and in BoaA, BoaB, BpaA, BpaB, and BpaF, they contain repeats of 11 [SLSTSTSTGTG], 14 [SLSTGLSTTNS(N/T/S)(V/L)(A/T)], and 18 [SLSTSTSTGLSSA(N/T/Q)SS(I/V)A] amino acids.

	Extended Signal Peptide			Signal Peptide	
	N1	H1	N2	H2	C
BoaA	MNKIYRKV	WNKARGQLVASELA	SSRSSVGEASVDAGR	SGDRTASAAFASEERNPGSGRMIPAMGAMLMFSTP	AWA-AL
BoaB	MNKIFRVI	WCRVKAACVVVSEEA	CLRGKK	SHSCRQGSRAAGEESVRFALSSIALAACILIGSLGSTLP	AVA-GT
BpaA	MNRSYRSI	WNEALGAWVAASEIS	SARGKPNK	SAVAKVVTAAVLAVVVQA	AHA-ST
BpaB	MNKTYRVS	WSASRGAWMAPETA	RRGKG	GHSLTIVCAIASGLLLAAP	AWA-DT
BpaC	MNRIFKSI	WCEQRTTWVAASEHA	VARGGR	ASSVASAGGLEKVLKLSILGAASLIAMGVVGPFAEE	AMA-AN
BpaD	MNRF*RIGKLD*I	VRYGINRRGRGAENH	LGRQESSRFNMTPR	AALVTLLLAAWSAPSV	AQA-LH
BpaE	MNKIYNVV	WSRVGQLIAVSEFS	RSNGK	CSTTQVVTAAPGVAGRTAASGRSRPSWTKLGLMSLAVSAAMGCMATD	AAA-QI
BpaF	MNKIYKTI	WCETTRSWAVSEHA	NGKR	GGATAAATTSARPIWTRLRGISLAALAAFGLGLFASPA	AFA-QS
Hia	MNKIFNVI	WNVVQTQWVVSELT	RTHTK	CASATVAVAVLATLLSAT	VEA-NN
BcpA	MKNHRYRL	VFSRVHGLMVAVEET	ASSAGK	ASAGETRRTLDKRGVHVTRFALRFAAFAALIAAGAMPW	VHA-QI
FhaB	MNTNLYRL	VFSHVRGMLVPVSEH	CTVGNTFCGRTR	GQARSGARATSLSVAPNALAWALMLACTGLPLV	THA-QG

FIG 3 ESPRs of putative *B. pseudomallei* 1026b trimeric AT proteins. Extended signal peptides and conventional signal peptides are indicated. N1, N-terminal charged region of the ESPR; H1, C-terminal hydrophobic region of the ESPR; N2, N-terminal charged region of the conventional signal peptide; H2, central hydrophobic region of the conventional signal peptide; C, signal peptidase recognition site, with putative cleavage site indicated with a hyphen. The N1, H1, N2, H2, and C regions were defined as described previously (41). For BpaD, "V" indicates the predicted start codon.

these regions begin with the sequence MN(K/R) and resemble the ESPRs of other trimeric AT and two-partner secretion proteins (Fig. 3). ESPRs can be found in ~10% of ATs and may be involved in regulating the translocation of ATs across the inner membrane into the periplasm (23, 41). Although BpaD as annotated does not contain an ESPR, manually translating the sequence immediately 5' of the *bpaD* ORF reveals codons for an MNR consensus sequence beginning 14 amino acids N-terminal to the predicted valine start codon. However, between the MNR and initial valine codons are two UGA stop codons, preventing the ESPR-like region from being translated. Therefore, it appears that BpaD, which is predicted to be the smallest of the trimeric ATs in *B. pseudomallei*, may have had an ESPR earlier in its evolutionary history (Fig. 3).

We used the domain annotation of trimeric autotransporter adhesins (daTAA) software to predict motifs within the passenger domains of *B. pseudomallei* trimeric AT proteins that have been described previously for other trimeric ATs (42). One particular repeated sequence, the YadA-like head motif (also known as the NSVAIG-S motif), is present in all eight proteins, making up the majority of the passenger domains of BpaC and BpaD (Fig. 2). This motif has been implicated in YadA-dependent collagen binding in *Yersinia enterocolitica*, though its role in *B. pseudomallei* adherence and/or virulence has not been assessed (43).

Five of the putative trimeric AT proteins (BoaA, BoaB, BpaA, BpaB, and BpaF) possess repeat regions in the passenger domain that are not common outside *Burkholderia* species and that share the N-terminal amino acid sequence SLST. These repeats are 11, 14, and 18 amino acids long, with consensus sequences of SLSTS TSTGTG, SLSTGLSTTNS(N/T/S)(V/L)(A/T), and SLSTSTSTGL SSA(N/T/Q)SS(I/V)A, respectively. A large portion of the passenger domains of BoaA and BoaB and nearly the entire passenger domains of BpaA and BpaF are composed of SLST repeats; however, searches for both primary amino acid sequence and secondary structure homologies fail to suggest a structure or function for these repeats. In strain 1026b, BoaA and BoaB are 63.1% identical and share similarly annotated regions within their passenger domains, perhaps suggesting that BoaA and BoaB are the result of a gene duplication event.

Construction of mutant strains. To evaluate the contributions of putative trimeric ATs to *B. pseudomallei* virulence, we constructed strains containing plasmid disruption and/or deletion mutations in each AT-encoding gene, as well as in the ORF(s) 3' of two AT-encoding gene loci (Fig. 4). Plasmid disruptions were

made such that the suicide plasmid pCC carrying an internal fragment of the AT-encoding gene (or of the gene 3' of *bpaE*) integrated at approximately the midpoint of the coding region of each gene via single-crossover homologous recombination. The presence of *nptII* (encoding a Km resistance protein) on the plasmid allowed for selection of cointegrants, and plating the strains on selective and nonselective media provided a means to assess the presence of the plasmid.

To test the stability of chromosomal integration of the disruption plasmids, we grew the disruption mutation strains in LSLB without Km and determined the percentage of cells that had retained (Km^r) or lost (Km^s) the plasmid after 48 h of incubation at 37°C. There was no significant plasmid loss for seven of eight AT-encoding gene disruption mutants or for Bp340::pDbaaE (Table 2). However, nearly all (97%) Bp340::pDbaaB cells had lost the plasmid after 24 h, suggesting that either the truncated BoaB' polypeptide interferes with growth *in vitro* or the plasmid is simply unstable in this location.

Because the plasmid instability observed for Bp340::pDbaaB prevented the use of this strain in subsequent assays, we constructed an unmarked, in-frame deletion mutation of *boaB* by using the allelic exchange plasmid pEXKm5, which has been used previously in *Burkholderia* spp. (32). We also created strains with in-frame deletion mutations in *bpaE*, *bpaF*, and a region encompassing both genes 3' of *bpaF* (Fig. 4). We chose to delete the two genes 3' of *bpaF* due to their unique presence in *Burkholderia* and their predicted function as glycosyltransferase genes, as glycosylation is a critical posttranslational modification of certain ATs (44).

One *B. pseudomallei* trimeric AT, BpaE, contributes to plaque formation in A549 cells. *B. pseudomallei* can spread from cell to cell without exiting the cytoplasm and can form plaques in a cell monolayer (35, 45, 46). *In vitro*, this process can be quantified by assessing the ability of *B. pseudomallei* to form plaques in a monolayer of cultured cells. We evaluated strains containing disruption mutations in seven of the eight putative trimeric AT-encoding genes (all but *boaB*) for plaque formation compared to that of the wild-type strain, Bp340 (Fig. 5A). Six of the seven disruption mutants formed plaques at a frequency similar to that of Bp340, which formed approximately 75 plaques per well. Bp340::pDbaaE, however, formed significantly fewer plaques than Bp340 (15.5 ± 3.26 compared to 78.5 ± 4.39 ; $P < 0.01$). We likewise evaluated plaque formation by the *boaB* deletion mutant but did not observe a difference compared to that by Bp340 (Fig. 5B). Our results suggest that BpaE and/or the OmpA family protein encoded by

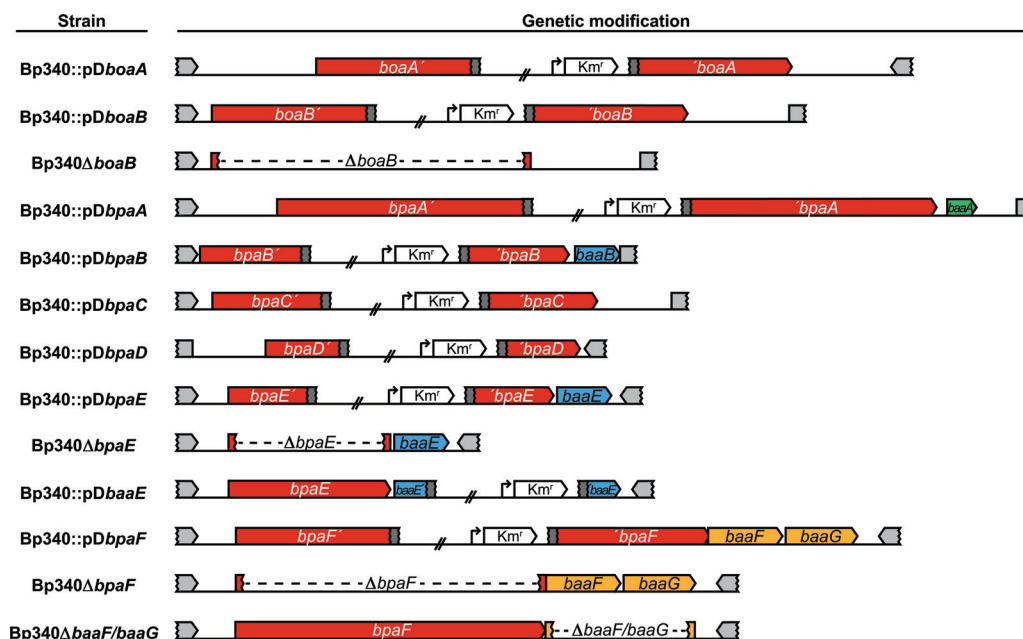


FIG 4 Schematic of deletion and disruption mutations used in this study.

baaE is required for one or more steps in the plaque formation process, which include adherence, invasion, intracellular survival, and cell-cell fusion.

All trimeric ATs tested, except BpaF, contribute to *B. pseudomallei* adherence to A549 cells. The plaques formed by Bp340::pDbpaE appeared to be similar in size to those formed by Bp340, suggesting that *bpaE* and/or *baaE* might be involved in plaque formation at a step prior to cell-cell fusion. We evaluated all seven disruption mutants and Bp340 Δ *boaB* for adherence to A549 cells as described in Materials and Methods. We plated the A549 cell lysates on LSLB agar without Km selection to determine the total number of adherent bacteria and on LSLB/Km agar to determine the number of adherent bacteria that still contained the cointegrated plasmid. For all disruption mutants, the number of Km^r CFU recovered was lower than the total number of CFU recovered, and the difference was especially dramatic for Bp340::pDbpaC, Bp340::pDbpaE, and Bp340::pDbpaF (Fig. 6A). Compared with the approximately 95% retention of the plasmid after 24 h of growth *in vitro*, these data indicate a strong selection for

bacteria that had lost the plasmid via homologous recombination (hence reverting to the wild type) in the assay. In all cases except Bp340::pDbpaF, the number of Km^r (i.e., mutant) CFU recovered from the A549 cells was significantly decreased compared to that

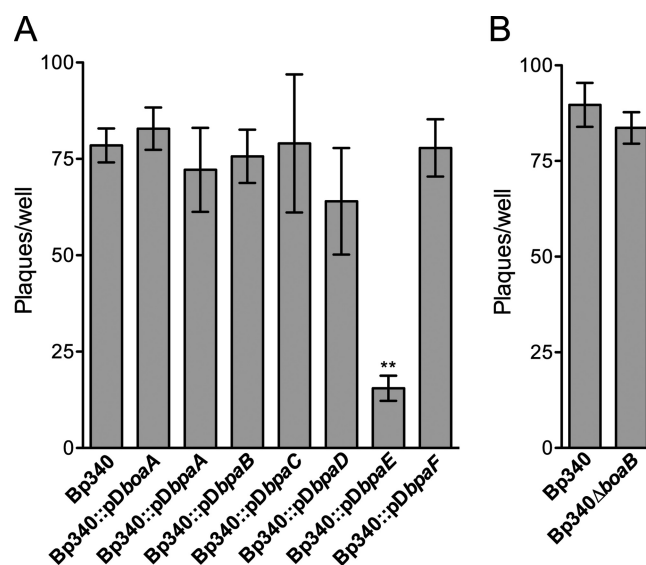


FIG 5 Plaque formation by *B. pseudomallei* 1026b trimeric AT disruption mutants. A549 cells (approximately 1×10^6 cells per well in a 6-well plate) were inoculated with *B. pseudomallei* trimeric AT disruption mutants at an MOI of 0.1, and plates were incubated for 2 h at 37°C. Plates were washed thoroughly with fresh medium and were overlaid with a mixture containing F12K medium, low-melting-point agarose, gentamicin, and neutral red. Plates were incubated for 24 h at 37°C with 5% CO₂, and plaques in each well were enumerated. Data are means \pm standard errors of the means (SEM) for two sets of experiments (A and B) performed in triplicate. Significance of differences was determined relative to Bp340. **, $P < 0.01$ by Tukey's multiple-comparison test following one-way analysis of variance (ANOVA).

TABLE 2 Disruption of plasmid stability *in vitro*

Strain	% Plasmid loss ^a	
	24 h	48 h
Bp340::pCC1	3.33 \pm 0.43	5.62 \pm 1.03
Bp340::pCC2	97.03 \pm 0.82	ND
Bp340::pCC3	2.47 \pm 0.56	2.75 \pm 0.56
Bp340::pCC4	4.65 \pm 0.11	8.76 \pm 0.57
Bp340::pCC5	2.06 \pm 0.93	5.02 \pm 1.41
Bp340::pCC6	1.03 \pm 0.49	0.90 \pm 1.79
Bp340::pCC7	1.12 \pm 0.51	3.63 \pm 0.20
Bp340::pCCbaaE	-0.052 \pm 1.52	2.24 \pm 1.17
Bp340::pCC8	3.20 \pm 1.40	7.23 \pm 0.72

^a Percent plasmid loss after growth in LSLB without selection for the indicated period. ND, not done.

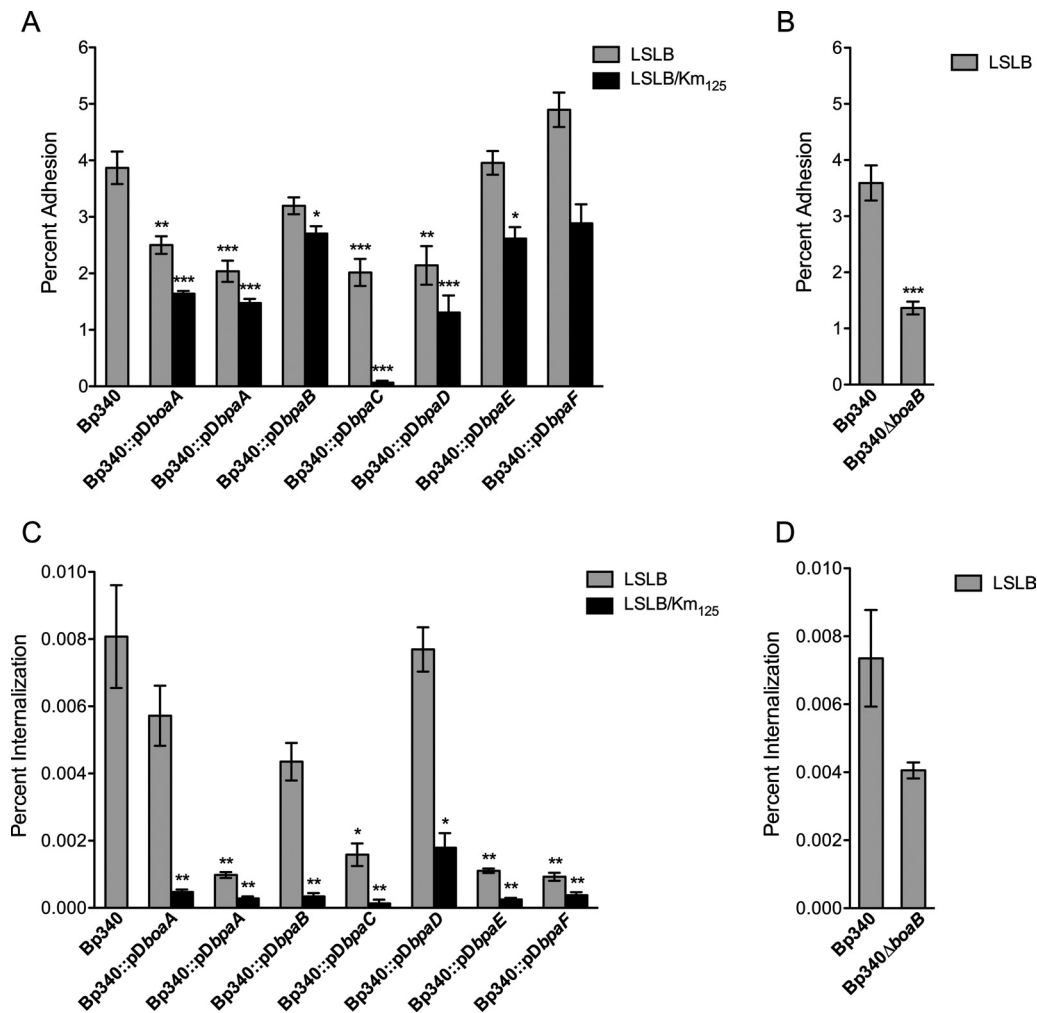


FIG 6 Contributions of trimeric AT proteins to adherence and invasion. A549 cells were grown as described for plaque formation experiments and were inoculated with the indicated strains at an MOI of 100. Plates were incubated for 2 h, and each well was washed thoroughly with fresh culture medium. For adherence of the trimeric AT disruption mutants (A) and Bp340 Δ boaB (B), cells were immediately lysed using 1% Triton X-100, and lysates were diluted and plated to determine the total number of CFU. For invasion of the trimeric AT disruption mutants (C) and Bp340 Δ boaB (D), cells were incubated for an additional 90 min in the presence of gentamicin, washed with fresh culture medium, and lysed using 1% Triton X-100. Lysates were diluted and plated to determine the total number of CFU. For both assays, lysates were plated on LSLB and LSLB containing Km to assess plasmid loss. Data are means \pm SEM for percentages of adherent or internalized bacteria compared to the inoculum and represent two experiments performed in triplicate. Significance of differences was determined relative to Bp340. *, $P < 0.05$; **, $P < 0.01$; ***, $P < 0.001$ by Tukey's multiple-comparison test following one-way ANOVA.

of Bp340. The number of CFU recovered for Bp340 Δ boaB was also significantly lower than that of the wild type (Fig. 6B). Taken together, our data suggest that all of the trimeric ATs tested and/or, in some cases, proteins encoded downstream, except BpaF, contribute to adherence to A549 cells.

All trimeric ATs tested, except BoaB, contribute to efficient internalization in A549 cells. Some trimeric AT proteins are known to be multifunctional, including *Proteus mirabilis* AipA and *Yersinia pseudotuberculosis* YadA, both of which function as adhesins and mediate entry into eukaryotic cells (47–49). To address the contribution of *B. pseudomallei* 1026b trimeric ATs to A549 cell internalization, we performed invasion assays with the seven disruption mutants and the *boaB* deletion mutant. Similar to the adherence assay results, the number of Km^r CFU recovered for each disruption mutant was lower (especially for Bp340::pDboaA, Bp340::pDboaB, and Bp340::pDboaD) than the total

number of CFU recovered, despite the stable integration of the plasmids observed *in vitro* (Fig. 6C and Table 2). Compared to Bp340, all seven disruption mutants were significantly attenuated in the ability to invade A549 cells, a phenotype at least somewhat due to internalization requiring initial bacterial adherence (Fig. 6C). Two of the strains severely deficient in internalization, i.e., Bp340::pDboaE and Bp340::pDboaF, displayed milder phenotypes in the adherence assay, suggesting that BpaE and BpaF (or the gene products encoded immediately 3' of *bpaE* and *bpaF*) may promote internalization apart from their apparent function as adhesins. The one deletion strain tested, Bp340 Δ boaB, was recovered at a level similar to that of Bp340 (Fig. 6D).

Evaluation of *B. pseudomallei* trimeric ATs in a mouse model of acute infection. The *B. pseudomallei* trimeric AT proteins BoaA and BoaB have been implicated in adherence to and invasion of host cells (21) (Fig. 6), but there has been no charac-

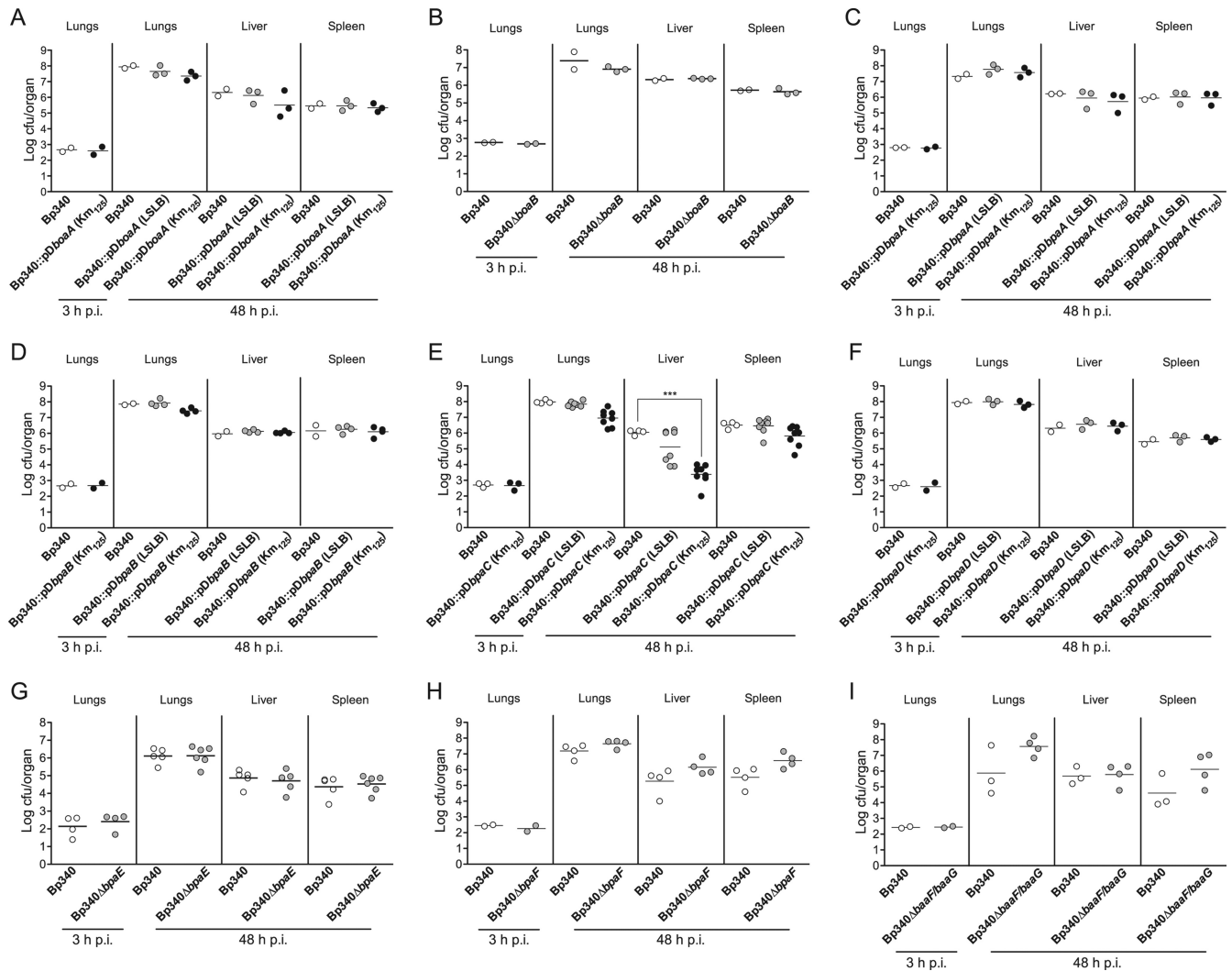


FIG 7 Contributions of *B. pseudomallei* 1026b trimeric ATs to virulence *in vivo*. Six- to 8-week-old female BALB/c mice were anesthetized with Avertin by intraperitoneal injection and were inoculated intranasally with 500 CFU of *B. pseudomallei* trimeric AT disruption (A, C, and D to F) and deletion (B and G to I) mutation strains. Mice were euthanized by CO₂ overdose at the indicated time points, and the lungs, liver, and spleen were aseptically harvested and homogenized. For each organ, the bacterial burden was determined by plating serial dilutions of the homogenates. For disruption mutants (A, C, and D to F), homogenates were plated on both LSLB and LSLB containing Km to assess plasmid loss. Significance of differences was determined relative to Bp340. **, $P < 0.01$; ***, $P < 0.001$ by Tukey's multiple-comparison test following one-way ANOVA.

terization of BoaA, Boab, or BpaA to -F in an animal model of *B. pseudomallei* infection. We hypothesized that one or more trimeric ATs would be required for *B. pseudomallei* virulence, consistent with the role of other trimeric ATs in virulence in a variety of Gram-negative pathogens (49–53). We infected BALB/c mice intranasally with 500 CFU of Bp340 or the trimeric AT-encoding gene disruption or deletion strains and then sacrificed the mice at 48 h postinoculation and determined bacterial burdens in the lungs, liver, and spleen. Mutants with plasmid disruptions of trimeric AT genes were plated on both LSLB and LSLB with 125 μ g/ml Km to assess plasmid loss *in vivo*.

At 48 h, the lungs of mice infected with Bp340 contained approximately 10^6 to 10^8 CFU, while the liver and spleen contained approximately 10^5 to 10^6 CFU of *B. pseudomallei* (Fig. 7). There was no significant difference in bacterial burden in any of the three organs for Bp340::pDboaA and Bp340 Δ boaB compared to Bp340

(Fig. 7A and B). Likewise, the burdens of Bp340::pDboaB, Bp340::pDboaC, and Bp340::pDboaD were not different from that of Bp340 in any of the organs (Fig. 7C, D, and F). Although the burden of Bp340::pDboaC was not different from that of Bp340 when cells were plated on LSLB in the absence of selection, there was significant plasmid loss in the liver, suggesting that this strain was defective in the ability to disseminate to or survive in this organ (Fig. 7). We did not observe any plasmid loss in the other disruption mutant strains, suggesting that there was a lack of selective pressure to have intact trimeric AT-encoding genes or any immediately 3' ORFs in this environment. At the time of sacrifice, all animals were moribund, regardless of infecting strain, indicating that the 50% lethal dose (LD₅₀) for each mutant strain was similar to that for Bp340 and less than the inoculum of 500 CFU.

To account for possible polar effects on the gene(s) 3' of bpaE and bpaF due to plasmid disruption of the trimeric AT-encoding

genes, we constructed in-frame deletion mutations in *bpaE* and *bpaF*, in anticipation that one or both encoded ATs would contribute to *B. pseudomallei* pathogenesis. We also constructed a strain with a disruption mutation in the gene 3' of *bpaE* (*baaE*) and a strain with an in-frame deletion in the genes 3' of *bpaF* (*baaF* and *baaG*). Both Bp340 $\Delta bpaE$ and Bp340 $\Delta bpaF$ were able to establish infection in the lung and to disseminate to the liver and spleen, similar to Bp340 (Fig. 7G and H). Additionally, neither Bp340::pDbaaE nor Bp340 $\Delta baaFG$ had a virulence defect (Fig. 7I and data not shown), suggesting that these highly conserved genes 3' of *bpaE* and *bpaF* are not required in the BALB/c intranasal model of infection.

DISCUSSION

In this study, we identified nine putative trimeric AT-encoding gene loci in the genome of *B. pseudomallei* clinical isolate 1026b and described the predicted domains of eight of the nine corresponding proteins (BimA excluded). We constructed strains containing disruption and/or deletion mutations in each of the AT-encoding genes and in genes immediately 3' of certain AT-encoding genes and then compared them with wild-type *B. pseudomallei* for plaque formation, adherence, and internalization in respiratory epithelial cells. Our characterization of eight trimeric ATs revealed that a majority of ATs and/or the proteins encoded downstream play a role in adherence to and invasion of A549 cells. Perhaps surprisingly, only BpaC played a role in virulence in the BALB/c mouse model of *B. pseudomallei* respiratory infection.

Nearly all AT proteins characterized so far have been shown to play roles in pathogenesis *in vivo* or in virulence-associated assays (24, 28, 49, 51, 54–56). Protein microarray and expression library studies have provided evidence that the majority of *B. pseudomallei* trimeric ATs are produced during human melioidosis (39, 57). A *B. pseudomallei* phage library expressed in *E. coli* revealed five AT proteins, BoaA, BpaB, BpaE, BpaF, and BimA, that reacted with convalescent-phase sera from melioidosis patients, indicating that these proteins were expressed at levels high enough to elicit an antibody response during infection (39). Additionally, a protein microarray study of potential antigens serodiagnostic for *B. pseudomallei* infection found that BpaA, BpaE, and BimA were significantly more reactive with melioidosis-positive patient sera than with melioidosis-negative control sera (57). These studies, along with the data presented here, support the hypothesis that most, if not all, trimeric ATs contribute to pathogenesis during human infection.

The *baaB* and *baaE* genes, located 3' of two of the AT-encoding genes characterized in this study (*bpaB* and *bpaE*), are predicted to encode OmpA family proteins, while the *baaA* gene, located 3' of *bpaA*, encodes a protein of unknown function. All three of these proteins are predicted to be lipidated and localized to the outer membrane, suggesting that they may function as accessory proteins for their corresponding ATs (and potentially for other ATs as well). The requirement of accessory proteins for translocation of ATs across the periplasm and insertion into the outer membrane was recently established as a general feature of AT biology (41, 58). The Bam complex, comprising the integral β -barrel protein BamA and the associated lipoproteins BamBCDE, is necessary for trimeric AT insertion in the outer membrane, through an unknown mechanism, while various periplasmic chaperones, such as SurA, Skp, and DegP, are required for AT passage through the

periplasm (41). Further characterization of the putative accessory proteins identified in our study will be necessary to determine their role, if any, in trimeric AT production and function.

Seven of the eight trimeric ATs included in our study possess ESPRs (Fig. 3). ESPRs were initially thought to function in cotranslational targeting of large type V family proteins to the periplasm; however, recent studies suggest that the region serves a more subtle function, by regulating the rate of translocation across the inner membrane to avoid an accumulation of misfolded proteins in the periplasm (41, 59, 60). Bioinformatic analyses have revealed that ESPRs appear to be restricted to type V proteins of $> \sim 100$ kDa in the *Beta*- and *Gamma*proteobacteria and are present in approximately 10% of AT proteins (23, 24, 41, 61). In *B. pseudomallei* 1026b, an uncharacteristically high 78% (seven of nine) of the trimeric ATs possess ESPRs, and the only two that lack such a feature are the two smallest trimeric ATs: BpaD and BimA. However, the fact that BpaD has what appears to be an ESPR remnant (Fig. 3) leads us to speculate that the ESPR is not necessary to regulate the secretion of proteins of this size and was thus lost as BpaD evolved.

In addition to the presence of ESPRs in the majority of trimeric ATs in *B. pseudomallei* 1026b, five of these proteins contain SLST repeats of 11, 14, or 18 aa that are unique to *Burkholderia* species and have no predicted structure or function. Not surprisingly, variation in the lengths of BoaA, BoaB, BpaA, BpaB, and BpaF homologs among *B. pseudomallei* strains is due largely to different numbers of SLST repeats in the passenger domain. It is possible, therefore, that within 1026b, the addition or loss of these repeats is used by the cell to regulate the length of the passenger domain and is perhaps related to AT function. Another possibility is that the serine- and threonine-rich repeats are glycosylation sites. Though initially thought to be a posttranslational modification restricted to eukaryotes, protein glycosylation in prokaryotes has been documented extensively and is important for the function of several virulence factors, including the classical ATs Ag43 and AIDA-I in pathogenic *E. coli* (24, 44, 62, 63). For Ag43, it has been shown that serine- and threonine-rich regions of the passenger domain are multiply glycosylated with heptose residues and that the addition of these sugars is essential for binding to human-derived HEp-2 cells (63). In 1026b, the proteins encoded by *baaF* and *baaG*, which are located immediately 3' of *bpaF*, have no predicted function based on homology searches of primary aa sequences, but structural homology searches revealed the greatest similarity to an *N*-acetylglucosamine transferase from the plant pathogen *Xanthomonas campestris*. Although we did not observe a phenotype *in vivo* for the mutant lacking both *baaF* and *baaG*, we are currently investigating the glycosylation state of BpaF and other AT proteins containing SLST repeats, as these genes may be important for AT function in other models.

In our study, we observed a significant decrease in the number of plaques formed on an A549 cell monolayer for only one trimeric AT-encoding gene disruption strain, Bp340::pD**bpaE**, compared to the wild-type strain. Though they were rarer, plaques formed by Bp340::pD**bpaE** were the same size as those formed by Bp340, indicating that once bacteria were inside the host cell, movement between cells was not hindered by loss of *bpaE* or *baaE*. The fact that six of the seven disruption mutants did not show a plaque formation defect suggests that either these genes are not important for any step in plaque formation (adherence, invasion, intracellular survival, and cell-cell fusion) or the disruption plas-

mid was lost due to selective pressure to maintain an intact trimeric AT-encoding gene. Plasmid loss could occur in the plaque assay, as it was performed in the absence of Km (Km was added to the medium to kill extracellular bacteria, and once inside the A549 cells, Km would be ineffective because it does not cross the cell membrane). It is difficult to recover bacteria from plaques (especially in a BSL3 laboratory) to determine the amount of plasmid loss during the formation of plaques; therefore, we performed adherence and invasion assays to assess the contributions of trimeric ATs to individual steps in the plaque formation process.

Our adherence and invasion assay data suggest that most trimeric AT proteins and/or, in some cases, the proteins encoded downstream contribute to these processes. When bacteria were grown *in vitro* without antibiotic selection for 24 h, only approximately 1 to 5% of the bacteria had lost the integrated plasmid. In the adherence assay used in our study, approximately 4% of the wild-type *B. pseudomallei* bacteria adhered to A549 cells within the 2-h incubation period. For most of the mutants, the percent adherent bacteria was below 4%, but the proportion of those that had lost the plasmid (and hence were genetically identical to Bp340) was relatively large. These data suggest that the adherence assay selected for bacteria that had lost the plasmid and therefore provide strong evidence that the AT proteins and/or the proteins encoded downstream of them are required for efficient adherence to and invasion of A549 cells. This conclusion is strengthened by the fact that in nearly all cases, almost no plasmid loss occurred in bacteria recovered from the lungs, livers, and spleens of mice that had been infected for 48 h with the various mutants.

Given the phenotypes displayed by the mutants in the plaque, adherence, and invasion assays, we expected to observe a role in pathogenesis for more than one trimeric AT in a BALB/c mouse model of infection. Instead, our animal experiments revealed a role only for *bpaC* in dissemination to or growth in the liver. Rather than providing a true reflection of the roles of the various AT proteins in infection, our data may reflect the limitations of the BALB/c respiratory infection model. Different animal models have yielded substantially different results with regard to flagella, one of the few *B. pseudomallei* virulence factors that has been examined in detail. DeShazer et al. initially characterized the *fliC* gene, encoding the flagellum structural protein, in *B. pseudomallei* 1026b and reported no difference in virulence for a *fliC* transposon mutant compared to the wild-type strain in either a diabetic rat or Syrian hamster model (29). However, they were careful to note that their results applied only to the two models they tested. In a more recent study, a $\Delta fliC$ mutant strain was evaluated in BALB/c mice inoculated by the intranasal route, and the mutant strain was dramatically attenuated for virulence compared to the wild-type strain, though it did not show a phenotype in an *in vitro* cell invasion assay or in the *Caenorhabditis elegans* model (64). Even within the same species, the choice of host strain can have profound consequences on the course of infection with *B. pseudomallei*. A study analyzing *B. pseudomallei* virulence in two mouse backgrounds, BALB/c and C57BL/6, found the difference in 10-day LD₅₀ values between the backgrounds to be nearly 4 orders of magnitude (65). When infected at the same dose, all BALB/c mice had to be sacrificed after 5 days, whereas all C57BL/6 mice survived until the experiment was terminated at 4 weeks (65). These observations suggest that comparing our mutant strains in an expanded number of animal models may reveal roles

for the various AT proteins that cannot be appreciated in BALB/c mice due to their extreme sensitivity to *B. pseudomallei*.

Our study is the first to systematically evaluate a class of genes (those encoding trimeric ATs) in *B. pseudomallei* both *in vitro* and *in vivo*. While we demonstrated that nearly all ATs tested have a function in adherence and/or invasion and that BpaC is important for efficient dissemination to or survival in the liver, we evaluated only strains in which a single trimeric AT-encoding gene was disrupted or deleted, and our analysis *in vivo* was limited to a single animal model and route of infection. It is probable that the deletion or disruption of two, three, or more AT-encoding genes will result in reduced virulence, and performing such studies would likely reveal redundant or synergistic functions for some ATs in infection. Because *B. pseudomallei* not only infects animals but also can be found in the rhizosphere, and even within the roots and foliage of several plant species (66), a full understanding of the roles of trimeric ATs may require the use of diverse eukaryotic host models.

ACKNOWLEDGMENTS

We thank Herbert Schweizer for providing us with *B. pseudomallei* strains and genetic tools. We also thank Michael Henderson and Sharon Taft-Benz for their technical assistance in the BSL3 lab.

This work was supported by a PSWRCE grant (U54 AI065359).

REFERENCES

1. Chaowagul W, White NJ, Dance DA, Wattanagoon Y, Naigowit P, Davis TM, Looareesuwan S, Pitakwatchara N. 1989. Melioidosis: a major cause of community-acquired septicemia in northeastern Thailand. *J. Infect. Dis.* 159:890–899.
2. White NJ. 2003. Melioidosis. *Lancet* 361:1715–1722.
3. Currie BJ, Fisher DA, Howard DM, Burrow JNC, Lo D, Selva-Nayagam S, Anstey NM, Huffam SE, Snelling PL, Marks PJ, Stephens DP, Lum GD, Jacups SP, Krause VL. 2000. Endemic melioidosis in tropical northern Australia: a 10-year prospective study and review of the literature. *Clin. Infect. Dis.* 31:981–986.
4. Dance DA. 2000. Melioidosis as an emerging global problem. *Acta Trop.* 74:115–119.
5. Dance DA. 1991. Melioidosis: the tip of the iceberg? *Clin. Microbiol. Rev.* 4:52–60.
6. Moore RA, DeShazer D, Reckseidler S, Weissman A, Woods DE. 1999. Efflux-mediated aminoglycoside and macrolide resistance in *Burkholderia pseudomallei*. *Antimicrob. Agents Chemother.* 43:465–470.
7. Godfrey AJ, Wong S, Dance DA, Chaowagul W, Bryan LE. 1991. *Pseudomonas pseudomallei* resistance to beta-lactam antibiotics due to alterations in the chromosomally encoded beta-lactamase. *Antimicrob. Agents Chemother.* 35:1635–1640.
8. Jones AL, Beveridge TJ, Woods DE. 1996. Intracellular survival of *Burkholderia pseudomallei*. *Infect. Immun.* 64:782–790.
9. Kespichayawattana W, Rattanachetkul S, Wanun T, Utaisincharoen P, Sirisinha S. 2000. *Burkholderia pseudomallei* induces cell fusion and actin-associated membrane protrusion: a possible mechanism for cell-to-cell spreading. *Infect. Immun.* 68:5377–5384.
10. Cheng AC. 2010. Melioidosis: advances in diagnosis and treatment. *Curr. Opin. Infect. Dis.* 23:554–559.
11. Brown NF, Boddey JA, Flegg CP, Beacham IR. 2002. Adherence of *Burkholderia pseudomallei* cells to cultured human epithelial cell lines is regulated by growth temperature. *Infect. Immun.* 70:974–980.
12. Jones AL, DeShazer D, Woods DE. 1997. Identification and characterization of a two-component regulatory system involved in invasion of eukaryotic cells and heavy-metal resistance in *Burkholderia pseudomallei*. *Infect. Immun.* 65:4972–4977.
13. Kespichayawattana W, Intachote P, Utaisincharoen P, Sirisinha S. 2004. Virulent *Burkholderia pseudomallei* is more efficient than avirulent *Burkholderia thailandensis* in invasion of and adherence to cultured human epithelial cells. *Microb. Pathog.* 36:287–292.
14. Muangsombut V, Suparak S, Pumirat P, Damnin S, Vattanaviboon P, Thongboonkerd V, Korbisrisate S. 2008. Inactivation of *Burkholderia*

- pseudomallei* bsaQ results in decreased invasion efficiency and delayed escape of bacteria from endocytic vesicles. Arch. Microbiol. 190:623–631.
15. Stevens MP, Stevens JM, Jeng RL, Taylor LA, Wood MW, Hawes P, Monaghan P, Welch MD, Galyov EE. 2005. Identification of a bacterial factor required for actin-based motility of *Burkholderia pseudomallei*. Mol. Microbiol. 56:40–53.
 16. Burntack MN, Brett PJ, Nair V, Warawa JM, Woods DE, Gherardini FC. 2008. *Burkholderia pseudomallei* type III secretion system mutants exhibit delayed vacuolar escape phenotypes in RAW 264.7 murine macrophages. Infect. Immun. 76:2991–3000.
 17. Burntack MN, Brett PJ, Harding SV, Ngugi SA, Ribot WJ, Chantratita N, Scorpio A, Milne TS, Dean RE, Fritz DL, Peacock SJ, Prior JL, Atkins TP, DeShazer D. 2011. The cluster 1 type VI secretion system is a major virulence determinant in *Burkholderia pseudomallei*. Infect. Immun. 79: 1512–1525.
 18. Suparak S, Kespichayawattana W, Haque A, Easton A, Damnin S, Lertmemongkolchai G, Bancroft GJ, Korbsrisate S. 2005. Multinucleated giant cell formation and apoptosis in infected host cells is mediated by *Burkholderia pseudomallei* type III secretion protein BipB. J. Bacteriol. 187:6556–6560.
 19. Suwannasarn D, Mahawantung J, Chaowagul W, Limmthurotsakul D, Felgner PL, Davies H, Bancroft GJ, Titball RW, Lertmemongkolchai G. 2011. Human immune responses to *Burkholderia pseudomallei* characterized by protein microarray analysis. J. Infect. Dis. 203:1002–1011.
 20. Dowling AJ, Wilkinson PA, Holden MT, Quail MA, Bentley SD, Reger J, Waterfield NR, Titball RW, Ffrench-Constant RH. 2010. Genome-wide analysis reveals loci encoding anti-macrophage factors in the human pathogen *Burkholderia pseudomallei* K96243. PLoS One 5:e15693. doi:10.1371/journal.pone.0015693.
 21. Balder R, Lipski S, Lazarus JJ, Grose W, Wooten RM, Hogan RJ, Woods DE, Lafontaine ER. 2010. Identification of *Burkholderia mallei* and *Burkholderia pseudomallei* adhesins for human respiratory epithelial cells. BMC Microbiol. 10:250. doi:10.1186/1471-2180-10-250.
 22. Essex-Lopresti AE, Boddey JA, Thomas R, Smith MP, Hartley MG, Atkins T, Brown NF, Tsang CH, Peak IR, Hill J, Beacham IR, Titball RW. 2005. A type IV pilin, PilA, contributes to adherence of *Burkholderia pseudomallei* and virulence *in vivo*. Infect. Immun. 73:1260–1264.
 23. Dautin N, Bernstein HD. 2007. Protein secretion in gram-negative bacteria via the autotransporter pathway. Annu. Rev. Microbiol. 61:89–112.
 24. Henderson IR, Navarro-Garcia F, Desvaux M, Fernandez RC, Ala'Aldeen D. 2004. Type V protein secretion pathway: the autotransporter story. Microbiol. Mol. Biol. Rev. 68:692–744.
 25. Cotter SE, Surana NK, St. Geme JW, III. 2005. Trimeric autotransporters: a distinct subfamily of autotransporter proteins. Trends Microbiol. 13:199–205.
 26. Cotter SE, Surana NK, Grass S, St. Geme JW, III. 2006. Trimeric autotransporters require trimerization of the passenger domain for stability and adhesive activity. J. Bacteriol. 188:5400–5407.
 27. El Tahir Y, Skurnik M. 2001. YadA, the multifaceted *Yersinia* adhesin. Int. J. Med. Microbiol. 291:209–218.
 28. Laarmann S, Cutter D, Juehne T, Barenkamp SJ, St. Geme JW. 2002. The *Haemophilus influenzae* Hia autotransporter harbours two adhesive pockets that reside in the passenger domain and recognize the same host cell receptor. Mol. Microbiol. 46:731–743.
 29. DeShazer D, Brett PJ, Carlyon R, Woods DE. 1997. Mutagenesis of *Burkholderia pseudomallei* with Tn5-OT182: isolation of motility mutants and molecular characterization of the flagellin structural gene. J. Bacteriol. 179:2116–2125.
 30. Lazar Adler NR, Stevens JM, Stevens MP, Galyov EE. 2011. Autotransporters and their role in the virulence of *Burkholderia pseudomallei* and *Burkholderia mallei*. Front. Microbiol. 2:151. doi:10.3389/fmicb.2011.00151.
 31. Edwards TE, Phan I, Abendroth J, Dieterich SH, Masoudi A, Guo W, Hewitt SN, Kelley A, Leibly D, Brittnacher MJ, Staker BL, Miller SI, Van Voorhis WC, Myler PJ, Stewart LJ. 2010. Structure of a *Burkholderia pseudomallei* trimeric autotransporter adhesin head. PLoS One 5:e12803. doi:10.1371/journal.pone.0012803.
 32. Lopez CM, Rholl DA, Trunk LA, Schweizer HP. 2009. Versatile dual-technology system for markerless allele replacement in *Burkholderia pseudomallei*. Appl. Environ. Microbiol. 75:6496–6503.
 33. Mima T, Schweizer HP. 2010. The BpeAB-OprB efflux pump of *Burkholderia pseudomallei* 1026b does not play a role in quorum sensing, virulence factor production, or extrusion of aminoglycosides but is a broad-spectrum drug efflux system. Antimicrob. Agents Chemother. 54:3113–3120.
 34. Edwards RA, Keller LH, Schifferli DM. 1998. Improved allelic exchange vectors and their use to analyze 987P fimbria gene expression. Gene 207: 149–157.
 35. French CT, Toesca JJ, Wu Teslaa T-HT, Beaty SM, Wong W, Liu M, Schröder I, Chiou Teittel P-YMA, Miller JF. 2011. Dissection of the *Burkholderia* intracellular life cycle using a photothermal nanoblade. Proc. Natl. Acad. Sci. U. S. A. 108:12095–12100.
 36. Utaisincharoen P, Arjcharoen S, Lengwehasatit I, Limposuwan K, Sirisinha S. 2005. *Burkholderia pseudomallei* invasion and activation of epithelial cells requires activation of p38 mitogen-activated protein kinase. Microb. Pathog. 38:107–112.
 37. Babu MM, Priya ML, Selvan AT, Madera M, Gough J, Aravind L, Sankaran K. 2006. A database of bacterial lipoproteins (DOLOP) with functional assignments to predicted lipoproteins. J. Bacteriol. 188:2761–2773.
 38. Okuda S, Tokuda H. 2011. Lipoprotein sorting in bacteria. Annu. Rev. Microbiol. 65:239–259.
 39. Tiyaawitsuri R, Holden MT, Tumapa S, Rengpipat S, Clarke SR, Foster SJ, Niernan WC, Day NP, Peacock SJ. 2007. *Burkholderia* Hep_Hag autotransporter (BuHA) proteins elicit a strong antibody response during experimental glanders but not human melioidosis. BMC Microbiol. 7:19. doi:10.1186/1471-2180-7-19.
 40. Holden MTG, Titball RW, Peacock SJ, Cerdeño-Tárraga AM, Atkins T, Crossman LC, Pitt T, Churcher C, Mungall K, Bentley SD, Sebahia M, Thomson NR, Bason N, Beacham IR, Brooks K, Brown KA, Brown NF, Challis GL, Cherevach I, Chillingworth T, Cronin A, Crossett B, Davis P, DeShazer D, Feltwell T, Fraser A, Hance Z, Hauser H, Holroyd S, Jagels K, Keith KE, Maddison M, Moule S, Price C, Quail MA, Rabinowitsch E, Rutherford K, Sanders M, Simmonds M, Songsivilai S, Stevens K, Tumapa S, Vesaratchavet M, Whitehead S, Yeats C, Barrell BG, Oyston PCF, Parkhill J. 2004. Genomic plasticity of the causative agent of melioidosis, *Burkholderia pseudomallei*. Proc. Natl. Acad. Sci. U. S. A. 101:14240–14245.
 41. Leyton DL, Rossiter AE, Henderson IR. 2012. From self sufficiency to dependence: mechanisms and factors important for autotransporter biogenesis. Nat. Rev. Microbiol. 10:213–225.
 42. Szczesny P, Lupas A. 2008. Domain annotation of trimeric autotransporter adhesins—daTAA. Bioinformatics 24:1251–1256.
 43. Tahir YE, Kuusela P, Skurnik M. 2000. Functional mapping of the *Yersinia enterocolitica* adhesin YadA. Identification of eight NSVAIG-S motifs in the amino-terminal half of the protein involved in collagen binding. Mol. Microbiol. 37:192–206.
 44. Benz I, Schmidt MA. 2001. Glycosylation with heptose residues mediated by the *aah* gene product is essential for adherence of the AIDA-I adhesin. Mol. Microbiol. 40:1403–1413.
 45. Galyov EE, Brett PJ, DeShazer D. 2010. Molecular insights into *Burkholderia pseudomallei* and *Burkholderia mallei* pathogenesis. Annu. Rev. Microbiol. 64:495–517.
 46. Pilatz S, Breitbach K, Hein N, Fehllhaber B, Schulze J, Brenneke B, Eberl L, Steinmetz I. 2006. Identification of *Burkholderia pseudomallei* genes required for the intracellular life cycle and *in vivo* virulence. Infect. Immun. 74:3576–3586.
 47. Bliska JB, Copass MC, Falkow S. 1993. The *Yersinia pseudotuberculosis* adhesin YadA mediates intimate bacterial attachment to and entry into HEp-2 cells. Infect. Immun. 61:3914–3921.
 48. Yang Y, Isberg RR. 1993. Cellular internalization in the absence of invasive expression is promoted by the *Yersinia pseudotuberculosis* *yadA* product. Infect. Immun. 61:3907–3913.
 49. Alamuri P, Lower M, Hiss JA, Himpel SD, Schneider G, Mobley HL. 2010. Adhesion, invasion, and agglutination mediated by two trimeric autotransporters in the human uropathogen *Proteus mirabilis*. Infect. Immun. 78:4882–4894.
 50. Mil-Homens D, Fialho AM. 2012. A BCAM0223 mutant of *Burkholderia cenocepacia* is deficient in hemagglutination, serum resistance, adhesion to epithelial cells and virulence. PLoS One 7:e41747. doi:10.1371/journal.pone.0041747.
 51. Ruiz-Ranwez V, Posadas DM, Van der Henst C, Estein SM, Arocena GM, Abdian PL, Martin FA, Sieira R, De Bolle X, Zorreguieta A. 2013. BtaE, an adhesin that belongs to the trimeric autotransporter family, is required for full virulence and defines a specific adhesive pole of *Brucella suis*. Infect. Immun. 81:996–1007.

52. Schutz M, Weiss EM, Schindler M, Hallstrom T, Zipfel PF, Linke D, Autenrieth IB. 2010. Trimer stability of YadA is critical for virulence of *Yersinia enterocolitica*. *Infect. Immun.* 78:2677–2690.
53. Bentancor LV, Camacho-Peiro A, Bozkurt-Guzel C, Pier GB, Maira-Litrán T. 2012. Identification of Ata, a multifunctional trimeric autotransporter of *Acinetobacter baumannii*. *J. Bacteriol.* 194:3950–3960.
54. Skurnik M, El Tahir Y, Saarinen M, Jalkanen S, Toivanen P. 1994. YadA mediates specific binding of enteropathogenic *Yersinia enterocolitica* to human intestinal submucosa. *Infect. Immun.* 62:1252–1261.
55. Barenkamp SJ, St. Geme JW. 1996. Identification of a second family of high-molecular-weight adhesion proteins expressed by non-typable *Haemophilus influenzae*. *Mol. Microbiol.* 19:1215–1223.
56. Hill DJ, Virji M. 2003. A novel cell-binding mechanism of *Moraxella catarrhalis* ubiquitous surface protein UspA: specific targeting of the N-domain of carcinoembryonic antigen-related cell adhesion molecules by UspA1. *Mol. Microbiol.* 48:117–129.
57. Felgner PL, Kayala MA, Vigil A, Burk C, Nakajima-Sasaki R, Pablo J, Molina DM, Hirst S, Chew JS, Wang D, Tan G, Duffield M, Yang R, Neel J, Chantratita N, Bancroft G, Lertmemongkolkhai G, Davies DH, Baldi P, Peacock S, Titball RW. 2009. A *Burkholderia pseudomallei* protein microarray reveals serodiagnostic and cross-reactive antigens. *Proc. Natl. Acad. Sci. U. S. A.* 106:13499–13504.
58. Ruiz-Perez F, Henderson IR, Leyton DL, Rossiter AE, Zhang Y, Nataro JP. 2009. Roles of periplasmic chaperone proteins in the biogenesis of serine protease autotransporters of *Enterobacteriaceae*. *J. Bacteriol.* 191: 6571–6583.
59. Desvaux M, Scott-Tucker A, Turner SM, Cooper LM, Huber D, Nataro JP, Henderson IR. 2007. A conserved extended signal peptide region directs posttranslational protein translocation via a novel mechanism. *Microbiology* 153:59–70.
60. Szabady RL, Peterson JH, Skillman KM, Bernstein HD. 2005. An unusual signal peptide facilitates late steps in the biogenesis of a bacterial autotransporter. *Proc. Natl. Acad. Sci. U. S. A.* 102:221–226.
61. Desvaux ML, Cooper LM, Filenko NA, Scott-Tucker A, Turner SM, Cole JA, Henderson IR. 2006. The unusual extended signal peptide region of the type V secretion system is phylogenetically restricted. *FEMS Microbiol. Lett.* 264:22–30.
62. Benz I, Schmidt MA. 2002. Never say never again: protein glycosylation in pathogenic bacteria. *Mol. Microbiol.* 45:267–276.
63. Sherlock O, Dobrindt U, Jensen JB, Munk Vejborg R, Klemm P. 2006. Glycosylation of the self-recognizing *Escherichia coli* Ag43 autotransporter protein. *J. Bacteriol.* 188:1798–1807.
64. Chua KL, Chan YY, Gan YH. 2003. Flagella are virulence determinants of *Burkholderia pseudomallei*. *Infect. Immun.* 71:1622–1629.
65. Leakey AK, Ulett GC, Hirst RG. 1998. BALB/c and C57BL/6 mice infected with virulent *Burkholderia pseudomallei* provide contrasting animal models for the acute and chronic forms of human melioidosis. *Microb. Pathog.* 24:269–275.
66. Kaestli M, Schmid M, Mayo M, Rothballer M, Harrington G, Richardson L, Hill A, Hill J, Tuanyok A, Keim P, Hartmann A, Currie BJ. 2012. Out of the ground: aerial and exotic habitats of the melioidosis bacterium *Burkholderia pseudomallei* in grasses in Australia. *Environ. Microbiol.* 14: 2058–2070.
67. Inatsuka CS, Xu Q, Vujkovic-Cvijin I, Wong S, Stibitz S, Miller JF, Cotter PA. 2010. Pertactin is required for *Bordetella* species to resist neutrophil-mediated clearance. *Infect. Immun.* 78:2901–2909.